

Defence Science Journal, Vol 48, No 1, January 1998, pp. 31-43  
© 1998, DESIDOC

## Structure of II-VI Lattice Mismatched Epilayers used for Blue-Green Lasers for Underwater Communication

K. Pinardi, H.E. Maes & S.C. Jain  
*IMEC, Kapeldreef 75, 3001 Leuven, Belgium.*

Uma Jain  
*Gargi College, University of Delhi, New Delhi - 110 049.*

and

M. Willander  
*Chalmers University of Technology and University of Gothenburg, S-41296 Göteborg, Sweden.*

### ABSTRACT

Critical thickness ( $h_c$ ) is calculated for capped and uncapped lattice mismatched II-VI semiconductor epilayers. Both the old equilibrium theory and the improved theory have been used. The calculated values are compared with the experimental data on epilayers of several II-VI semiconductors and alloys. The observed values of  $h_c$  are larger than the calculated values. However the discrepancy is much smaller than that found in *InGaAs/GaAs* and *GeSi/Si* layers. Moreover as compared to *InGaAs/GaAs* and *GeSi/Si* layers, the experimental data show a much smaller scatter and can be fitted with one curve. Strain relaxation in layers with thickness  $h > h_c$  is also calculated. Strain relaxation in *ZnSe* layers grown on (100) *GaAs* shows good agreement with the equilibrium theory. In other cases the observed relaxation is sluggish, the residual strain is larger than its calculated value. Thick highly mismatched layers behave differently. The residual strain agrees with theory and dislocations are distributed periodically. A model to interpret these observations is suggested. Implications of this study on the stability of II-VI strained layers are discussed.

### 1. INTRODUCTION

At present, commercial semiconductor lasers are based on *GaAs* or alloys of *GaAs* and other III-V semiconductors. *GaAs* device technology is quite mature and the efficiency of these lasers for conversion of electrons to monochromatic photons is high<sup>1</sup>. However they can emit coherent radiation only in the infrared and red regions of spectrum.

The emitted radiation depends on the band gap of the semiconductor. III-V semiconductors cannot be used to fabricate light emitting diodes (LEDs) or laser diodes (LDs) for emission of light at shorter wavelengths (in the blue and green regions of the spectrum) because their band gaps are not sufficiently large. Green-light sources are needed for underwater communication in defence. Short

Received 11 June 1997

wavelength LEDs and lasers are also important for many other applications<sup>1,2</sup>. They are useful in medical diagnostics and for fabricating red-green-blue display devices. In compact disc reading application, the density of the data stored on the disc can increase from 650-2600 MB if short-wavelength lasers are used<sup>1,2</sup>. Until recently, only gas lasers ( $Ar^+$  laser) could emit light in the short wavelength region. The gas lasers are large in size and are not suitable for the above mentioned applications. Recently II-VI semiconductor lasers have been fabricated which emit in the blue and green region<sup>1-4</sup>. Extensive work is being done on these lasers, and number of publications on emission of blue-green light from strained-layer superlattices of II-VI semiconductors are increasing rapidly<sup>5,6</sup>.  $ZnSe$  is an essential constituent in most short wavelength lasers fabricated so far. However, large single crystals of  $ZnSe$  are not yet available. Most II-VI devices fabricated so far used II-VI layers grown on  $GaAs$  substrate.  $ZnSe$  has a significant lattice mismatch with  $GaAs$  (values of lattice mismatch used in different papers are slightly different, e.g. 0.265 per cent<sup>7</sup>, 0.27 per cent<sup>8</sup> and 0.272 per cent<sup>9</sup>). The mismatch between  $GaAs$  and most other II-VI semiconductors (except  $MgS$ ) is large<sup>10</sup>. Both lattice constant and band gap of  $ZnSe$  can be adjusted by alloying it with  $ZnS$ ,  $CdS$ ,  $CdSe$ ,  $MgS$  and  $MgSe$ . In most cases, the alloy layers used in devices, have significant lattice mismatch with  $GaAs$  and are strained. Therefore, it is important to determine how stable these layers are. If the layers are not stable, long-term reliability of the lasers will be poor.

Critical thickness  $h_c$  and strain relaxation in  $Ge_xSi_{1-x}/Si$  and  $In_xGa_{1-x}As/GaAs$  epilayers have been studied extensively<sup>11-14</sup>. Comparison of the experimental results on  $GeSi$  and  $InGaAs$  with the equilibrium theory show large discrepancies. The theory of the critical thickness and strain relaxation has been improved<sup>15-17</sup>, but the discrepancy between the theory and the experiments on  $GeSi$  and  $InGaAs$  still persists. Work on the measurement of critical thickness and strain relaxation in epilayers of II-VI semiconductors was done in late 1980s.

Systematic experiments were performed and extensive data on different II-VI alloy layers were obtained. However only sporadic reports of comparison of data with theory have been published. Since, II-VI semiconductors are not as hard as  $GeSi/Si$  or  $InGaAs/GaAs$  layers (elastic constants  $C_{11}$  are 81 GPa for  $ZnSe$ , 71.3 GPa for  $ZnTe$ , and 53 GPa for  $CdTe$ <sup>18</sup> as compared to 166 GPa for  $Si$ <sup>19</sup> and 119 GPa for  $GaAs$ <sup>20</sup>) and the energy needed for nucleation and propagation of dislocations is smaller in II-VI layers<sup>21</sup>. It is interesting to examine whether the experimental results in II-VI semiconductors behave differently and agree with the theoretical results. It will help us to decide whether or not the II-VI epilayers are stable. As the thickness of the epilayers increases beyond  $h_c$ , the misfit dislocations are produced and strain relaxes by plastic deformation. The strain continues to relax as the thickness continues to increase until it saturates at a small residual value. Extensive experimental data on the strain relaxation on  $ZnSe$  is available but it has not been compared with the theoretical values. The values of  $h_c$  and strain relaxation in II-VI strained epilayers have been calculated and compared with the experimental values.

## 2. STRAIN & ENERGY OF STRAINED LAYERS

### 2.1 Misfit strain

Consider an epilayer of a semiconductor with lattice constant  $a_1$  grown on a thick substrate with lattice constant  $a_{sub}$  (Fig. 1). The lattice mismatch is measured by the misfit parameter  $f_m$  defined<sup>11</sup>.

$$f_m = \frac{a_1 - a_{sub}}{a_{sub}} \quad (1)$$

If both misfit parameter  $f_m$  and thickness  $h$  of the epilayer are small, the misfit between the two semiconductors is accommodated by a compressive tetragonal strain of the epilayer as shown in Fig. 1(a). The strain is homogeneous and is known as 'misfit strain', and the layer is pseudomorphic. For a given  $f_m$ , if thickness  $h$  of the epilayer exceeds a certain thickness, known as  $h_c$ , the strain is partly accommodated by the misfit

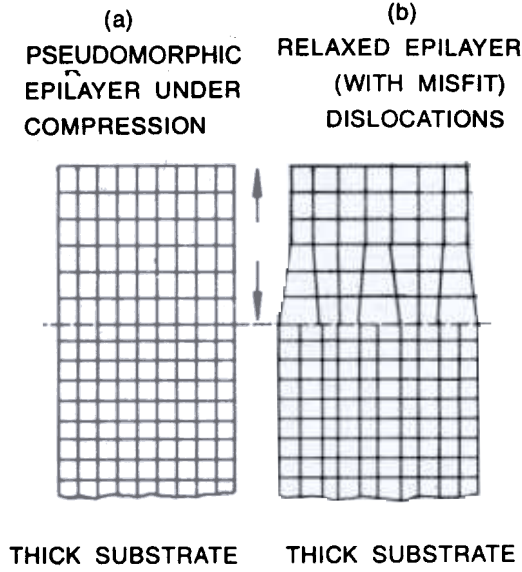


Figure 1. Structure of an epilayer under biaxial compression (a) pseudomorphic, and (b) relaxed with misfit dislocations. Dotted horizontal line represents the interface.

dislocations as shown in Fig. 1(b). The in-plane homogeneous strain in the pseudomorphic layer<sup>11</sup> is given by

$$\varepsilon_{\parallel} = -f_m \quad (2)$$

If the epilayer contains dislocations with average inter-dislocation  $p$ , the expression for strain becomes

$$\varepsilon_{\parallel} = -\left(f_m + \frac{b_1}{p}\right) \quad (3)$$

where

$$b_1 = -b \sin\alpha \sin\beta, \text{ and } b \text{ is the Burgers vector.}$$

For 60° dislocations

$$\alpha = \operatorname{arctan} \frac{1}{\sqrt{2}}, \quad \beta = \frac{\pi}{3} \quad (4)$$

and for 90° dislocations

$$\alpha = \frac{\pi}{2}, \quad \beta = \frac{\pi}{2} \quad (5)$$

Note that  $f_m$  and  $b_1/p$  have opposite signs and numerically  $b_1/p$  is always subtracted from  $f_m$  in Eqn (3). If the lattice constant of the layer is smaller than that of the substrate,  $f_m$  is negative and  $\varepsilon_{\parallel}$  is positive. According to this convention, tensile strain and stress are positive and compressive strain and stress are negative.

## 2.2 Energy of Strained Layers

The total energy  $E_T$  of partially relaxed layer contains the contributions<sup>11</sup>: (i) energy due to misfit strain; (ii) energy  $(b_1/f_m)^2$  due to the average (homogeneous) strain produced by the dislocation arrays; (iii) energy of interaction  $2f_m b_1/p$  between the average strain due to dislocation arrays and the homogeneous misfit strain; and (iv) energy  $E_{DS}$  (or  $E_{DS}^{cap}$  for the capped layer) due to fluctuating part of the strain of dislocation arrays. The fluctuating part has an average zero and therefore does not interact with the homogeneous strains. Using all contributions, the following expressions are obtained for the total energy (per unit area) of the uncapped layer<sup>11</sup>

$$E_T = E_H + \frac{2}{p} E_{DS} \quad (6)$$

where

$E_H$  is the energy corresponding to the first three contributions. The expression for  $E_H$  is

$$E_H = Bh \left(f_m + \frac{b_1}{p}\right)^2 \quad (7)$$

Where

$$B = 2\mu \frac{1+\nu}{1-\nu} \quad (8)$$

Here  $\nu$  is Poisson's ratio,  $\mu$  is the shear modulus of elasticity and  $h$  is the thickness of the layer. The expression for  $E_{DS}$  is

$$E_{DS} = A \left[ a_0 + a_1 \ln \left( p \frac{1-e^{-s}}{2\pi q} \right) + a_2 \frac{se-s}{1-e^{-s}} \right. \\ \left. \left[ -a_3 \frac{s^2 e^{-s}}{(1-e^{-s})^2} - a_2 \right] \right] \quad (9)$$

where

$$a_2 = b_1^2 - b_2^2, \quad s = 4\pi \frac{h}{p} \quad (10)$$

The constants used in Eqn (9) are defined as

$$A = \frac{\mu}{4\pi(1-\nu)} \quad (11)$$

$$b_1 = -b \sin \alpha \sin \beta, \quad b_2 = b \cos \alpha \sin \beta, \\ b_3 = -b \cos \beta \quad (12)$$

$$a_0 = (b_1^2 + b_2^2) \left( \sin^2 \alpha - \frac{1-2\nu}{4(1-\nu)} \right) \\ a_1 = (b_1^2 + b_2^2) + (1-\nu) b_3^2 \\ a_3 = \frac{1}{2} (b_1^2 + b_2^2) \quad (13)$$

Most strained layer heterostructure devices use unstrained layers on top of the strained layers. Such strained layers are known as capped or buried strained layers. If the cap is sufficiently thick, relaxation of strain occurs by the introduction of dislocation dipoles<sup>11,22</sup>. A dipole consists of a pair of dislocations, one each at the upper and lower interfaces. Schematic representations of a 60° array of dislocations in an uncapped layer and dipoles in a capped layer are shown in Fig. 2. Both dislocations and the dipoles are of 60° type and  $\alpha$  in the capped layer is the same as in the uncapped layers. The dislocations at the lower interface have a Burgers vector  $b$  and the upper interface, a Burgers vector  $-b$ . In this case the dipole spacing  $p$  is the spacing both in the upper and the lower array of dislocations (Fig. 2). Angle  $\theta$  is the angle between the line joining two dislocations of a dipole and perpendicular to the interface. The cap modifies the energy expressions of the dislocations as well as the magnitude and kinetics of strain relaxation. The total energy  $E_T$  of the capped layer can be calculated in a manner similar to that used above for the layer with free surface<sup>22</sup>. The expression for  $E_T^{cap}$  is

$$E_T^{cap} = E_H + \frac{2}{p} E_{DS}^{cap} \quad (14)$$

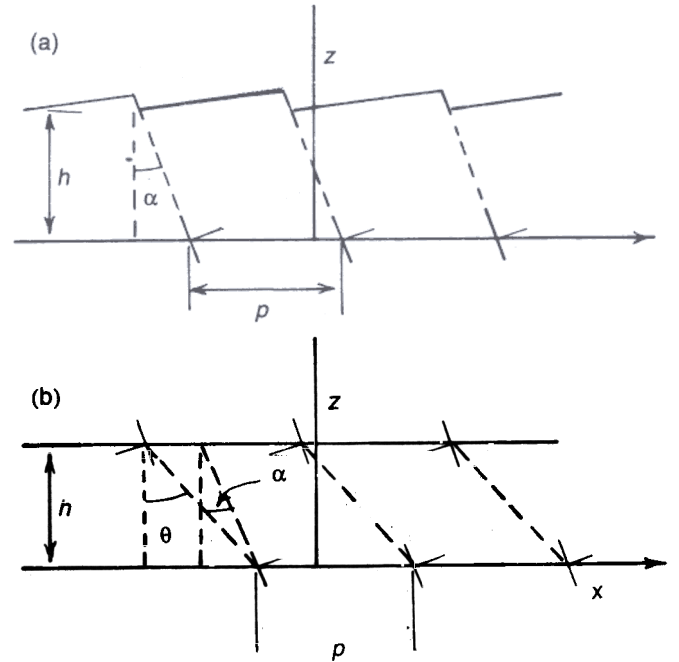


Figure 2. Schematic representation of (a) 60° dislocations in an uncapped layer, and (b) 60° dipoles in a capped layer.

The expression for  $E_{DS}^{cap}$  is

$$E_{DS}^{cap} = 2A \left[ 2a_4 + a_1 \operatorname{Re} \ln \left( p \frac{-e^{-w}}{1 - e^{-w}} \right) \right. \\ \left. \left[ -2a_3 w \operatorname{Re} \left( \frac{e^{-2i\alpha} e^{-w}}{1 - e^{-w}} + a_3 \right) \right] \right] \quad (15)$$

where

$$w = 2\pi \frac{h}{p}$$

$$a_4 = -\frac{1}{2} (b_1^2 + b_2^2) \frac{1-2\nu}{4(1-\nu)}$$

And

$$a_5 = (b_1^2 + b_2^2) \cos^2 \alpha \quad (16)$$

The expression for the total energy  $E_T$  of an uncapped layer used in Van der Merwe's theory is<sup>14,23</sup>

$$E_T^m = E_H + \frac{2}{p} E_D^{\infty} \quad (17)$$

Note that  $E_D^{\infty}$  is the dislocation energy for an isolated dislocation and it does not include into the dislocation interactions. The expression for  $E_D^{\infty}$  is

$$E_D^{\infty} = \frac{\mu b^2}{4\pi(1-\nu)} \left[ (1 - \nu \cos^2 \beta) \ln \frac{\rho_c h}{q} \right] \quad (18)$$

Here  $\rho_c$  is a parameter used to account for the non-elastic part of the core energy of dislocations\*, and  $q$  is the core radius of the dislocation line, usually taken to equal  $b/2$ . It is seen that the correct Eqn (6) for total energy is quite different from Eqn (17) used in the earlier work.

### 3. CRITICAL THICKNESS

#### 3.1 Theory

The force balance theory of Matthews and Blakeslee<sup>24</sup> and the theory of Van der Merwe<sup>23</sup> based on principle of energy minimisation has been discussed. It is concluded that contrary to widespread belief, the two theories are equivalent. Misfit dislocations are formed either by nucleation of surface half loops and their expansion as shown in Fig. 3(a) or by propagation of existing threading dislocations as shown in Fig. 3(b). In their force balance theory, Matthews and Blakeslee<sup>24</sup> considered a substrate-epilayer structure in which threading dislocations crossing the interface are present and move to deposit the misfit dislocations. The threading dislocation experiences two competing forces. When the threading dislocation propagates through the layer, a segment of misfit dislocation is created reducing the strain and the energy of the epilayer. This provides the driving force for the motion. The force is equal<sup>24</sup> to  $Bh f_m b_1$ . The line tension  $E_D^{\infty}$  (which is equal to the dislocation energy per unit length) of the misfit dislocation opposes the motion. The net force  $G$  acting on the threading dislocation is

$$G = Bh |f_m b_1| - E_D^{\infty} \quad (19)$$

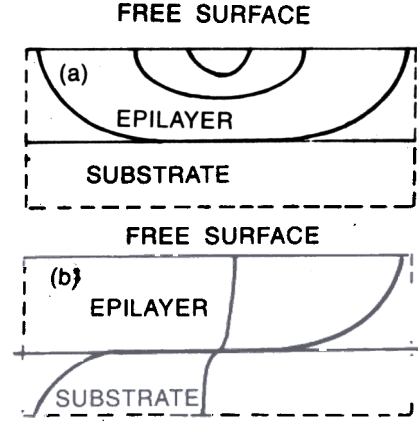


Figure 3. Generation of misfit dislocations (a) by nucleation and expansion of a surface half loop, and (b) by motion of an existing threading dislocation.

Below the  $h_c$ ,  $G$  is negative and the layer remains pseudomorphic. As  $h$  increases, the first term in Eqn (19) increases faster than the second term. Matthews and Blakeslee assumed that at  $h = h_c$ ,  $G = 0$ . For  $h > h_c$ ,  $G$  is positive and the threading dislocation moves, depositing the misfit dislocation. Equating  $G$  to 0, the Matthews and Blakeslee equation for  $h_c$  is obtained as

$$h_c = \frac{b^2 (1 - \nu \cos^2 \beta)}{8\pi f_m (1 + \nu) b_1} \ln \frac{\rho_c h_c}{q} \quad (20)$$

If the layer is covered with a thick cap layer of the same material as the substrate,  $h_c$  of the epilayer increases<sup>11</sup> by a factor of about 2. The principle of energy minimisation states that below  $h_c$ , the energy of the epilayer should increase by the introduction of the misfit dislocations and beyond  $h_c$ , the energy should decrease. At  $h_c$ , the total energy of the layer is minimum and the change in energy on introducing a dislocation is 0. We write an expression for the total energy of a sample of linear dimension  $L$  ( $L$  is large so that end effects are negligible) and equate its derivative (with respect to  $1/L$ ) to 0 to obtain the minimum energy. It can be seen that this leads to exactly the same equations viz.,  $G = 0$  for determining  $h_c$ .

Though Eqn (17) is not correct, exactly the same expression for  $h_c$  is obtained by equating to zero the first derivative of the total energy with

Values of  $\rho_c$  are not known with any certainty, and different values of this parameter have been used by different workers.

respect to  $1/p$  and letting  $p \rightarrow \infty$ . If Van der Merwe's approach is followed, but use correct expression (6) for the total energy, Eqn (20) is not obtained for  $h_c$ . In the correct theory, the value of  $h_c$  comes out to be different depending upon whether one considers introduction of a single dislocation or of arrays of  $60^\circ$  dislocations<sup>11</sup>. Cohen-Solal, *et al*<sup>25</sup>, have proposed a new model for calculating  $h_c$  of a lattice mismatched layer. The  $h_c$  is the thickness at which the homogeneous strain energy and the energy of the totally relaxed layer are equal. Energy was calculated using Keating's valence force field approximation. They found that the critical layer thickness can be written as

$$h_c = A^* f_m^{-3/2} \tag{21}$$

where  $A^*$  is an adjustable parameter. At  $h = h_c$ , there is considerable strain in the layer and the arguments leading to this equation are not sound. However by adjusting the parameter  $A^*$ , fit of Eqn (21) with experiments on II-VI semiconductor epilayers (Fig. 4) is reasonable.

**Table 1.** Observed values of  $h_c$ . The -ve sign indicates that the lattice constants of the over layer is smaller i.e.  $f_m$  is negative and the in-plane strain  $\epsilon_{||}$  is positive (Eqns (1) and (2))

Sample, $f_m$ (%)	Method	$h_c$ (nm)	T (°C)	Ref
ZnSe/GaAs, 0.272				
ZnSe/GaAs, 0.27				
ZnSe/ZnS <sup>1</sup> , 5			-	
ZnTe/GaAs, 7.5			250	
CdSe/ZnSe, (symmetrical SLS), 6.8				
ZnSe/CdSe, (symmetrical SLS), -6.3				
CdTe/Cd <sub>0.97</sub> Zn <sub>0.03</sub> Te, 0.18			-	
CdTe/ZnTe, 6			250, 320	
CdTe/Cd <sub>0.96</sub> Zn <sub>0.04</sub> Te, 0.23				
CdTe/InSb, 0.04				
CdTe/Cd <sub>1-x</sub> Zn <sub>x</sub> Te				
ZnTe/CdTe, -5.8	R		260	

Values in (111) orientation were somewhat smaller  
 2 Relaxed buffer  
 x X-ray diffraction  
 Ch Channeling

### 3.2 Experimental Values of Critical Thickness

Pinardi, *et al.* have compiled the experimental values of  $h_c$  of II-VI semiconductor and alloy epilayers (Table 1). The value of  $h_c$  of ZnSe/GaAs has been determined by many workers<sup>8,9,30</sup> Yokogawa, *et al*<sup>9</sup>, measured the lattice constants of ZnSe layers grown on GaAs substrates by metallo organic vapour phase epitaxy. Lattice mismatch for this system is 0.272 per cent. Taking  $\nu = 0.376$  and Burgers vector  $b = 4.008$ , and using Eqn (20), the calculated  $h_c$  comes out to be 21 nm as compared to the observed value of 150 nm. The difference between the calculated and the observed  $h_c$  was explained by assuming that there is an energy barrier for the creation of the misfit dislocations. Other authors<sup>8,30</sup> have also observed  $h_c = 150$  nm for ZnSe layers grown on GaAs. The  $h_c$  of ZnSe on ZnS (mismatch 5 %) buffer<sup>9</sup> is 5 nm. Fontaine, *et al*<sup>32</sup>, measured  $h_c$  of CdTe epilayers grown on InSb substrates and on Cd<sub>0.96</sub>Zn<sub>0.04</sub>Te substrates using X-ray diffraction method. Both (100) and (111) substrates were used. The separation of the X-ray peaks from the layer and the substrate is given by

$$a_s - a_L^\perp / a_s = -\Delta\theta / \tan\theta \tag{22}$$

R RHEED  
 RO RHEED Oscillations  
 T TEM

where  $a_L^\perp$  is the lattice constant of the layer in the growth direction. Using the measured values of the lattice constant  $a_L^\perp$  of the epilayer they found that stress was constant corresponding to a coherent layer up to a thickness of  $0.483 \mu\text{m}$  for a (111)  $\text{Cd}_{0.96}\text{Zn}_{0.04}$  substrate and  $0.513 \mu\text{m}$  for a (100)  $\text{Cd}_{0.96}\text{Zn}_{0.04}\text{Te}$  substrate. The corresponding values for  $\text{InSb}$  substrate are  $2.8 \mu\text{m}$  and  $2.95 \mu\text{m}$ . These values are shown in Table 1. The values for the (111) substrates are not given in Table 1.

Chami, *et al.*<sup>21</sup> have grown  $\text{CdTe}$  layers on a  $\text{Cd}_{0.97}\text{Zn}_{0.03}\text{Te}$  (mismatch 0.18 %) substrate by molecular beam epitaxy (MBE) and have studied the misfit dislocation density at the interface by channeling technique. The value of  $h_c$  was 390 nm. The formation energy of misfit dislocations was estimated to be  $10^{-8} \text{ J/m}$ . Bauer, *et al.*<sup>26</sup> investigated two samples, one in which the  $\text{ZnTe}$  layers were directly grown on  $\text{GaAs}$  and the other in which a pseudomorphic layer of  $\text{ZnSe}$  layer was deposited on  $\text{GaAs}$  and the  $\text{ZnTe}$  layer was deposited on  $\text{ZnSe}/\text{GaAs}$  (mismatch 7.5 %). The layers were characterised using *in situ* reflection high energy electron diffraction (RHEED), Raman shifts of the LO mode and high resolution transmission electron microscopy. The surface lattice constant (lattice constant in a plane parallel to the interface) was determined by RHEED streak separation. In both cases, the lattice constant of the  $\text{ZnTe}$  layers remained equal to that of  $\text{GaAs}$  up to a thickness of 12 Å suggesting that the experimental  $h_c$  of  $\text{ZnTe}$  on  $\text{GaAs}$  is 12 Å.

Extensive measurements of  $h_c$  of  $\text{CdTe}$  grown on  $\text{Cd}_x\text{Zn}_{1-x}\text{Te}$  have been made<sup>25</sup> and the values are shown by open circles in Fig. 4. Recently, similar data have been obtained by Cibert, *et al.*<sup>31</sup> (not shown in Fig. 4). The plot of Eqn (21) with  $A^* = 0.45 \text{ \AA}$  is shown by the dotted line in Fig. 4. The  $h_c$  of  $\text{ZnTe}$  on<sup>29</sup>  $\text{CdTe}$  is 2.1 nm. The  $h_c$  of  $\text{CdSe}$  and  $\text{ZnSe}$  have been measured in a symmetrical strained superlattice (SLS) and the values are 0.91 nm and 0.28 nm, respectively<sup>27</sup>. A summary of all observed values of  $h_c$  is given in Table 1. Pinardi, *et al.* have calculated  $h_c$  using Matthews and Blakeslee Eqn (20) for the II-VI semiconductors shown by the

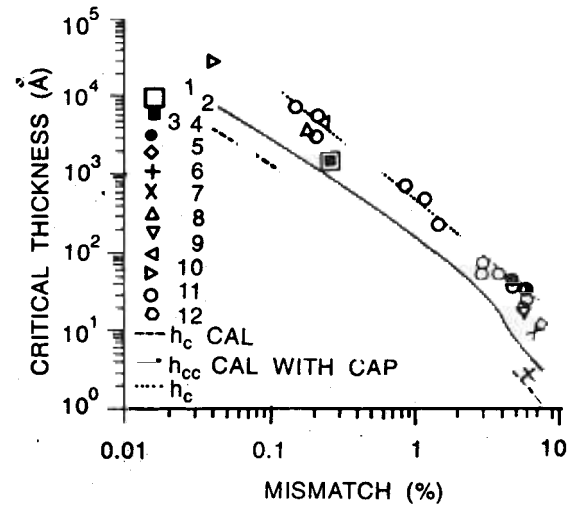


Figure 4. Critical thickness of II-VI semiconductor lattice mismatched layers. Dashed and solid lines give the calculated values of  $h_c$  for the layers with free surface and for the capped layers, respectively.

dashed line on Fig. 4. Pinardi, *et al.* have also calculated  $h_{cc}$  for the capped layers. The  $h_{cc}$  for the capped layers is shown by the solid curve. Authors have also calculated  $h_c$  using the improved theory as discussed. The values obtained by the improved theory are nearly equal to those shown in Fig. 4, the maximum difference being 0.3 per cent at low mismatch. The experimental data from Table 1 are also plotted in Fig. 4. Considering that experimental values are for many different II-VI semiconductor and alloy layers and that the experiments have been done in different laboratories, the scatter in the experimental values is rather small. For comparison, The experimental values of III-V layers have also been compiled and plotted. The scatter of experimental points is much larger in this case. The maximum discrepancy between the observed and the calculated values is also much larger for the III-V layers and for  $\text{GeSi}$  layers (not shown in the figure).

#### 4. STRAIN RELAXATION IN THICK EPILAYERS

Lu, *et al.*<sup>33</sup> have grown  $\text{ZnSe}$  layers on  $(\text{InGa})\text{P}$  buffers deposited on  $\text{GaAs}$  substrates by gas source MBE. By varying the composition of buffer layer, its lattice constant can be changed from that of  $\text{GaP}$  to that of  $\text{InP}$ . If the growth temperature was below

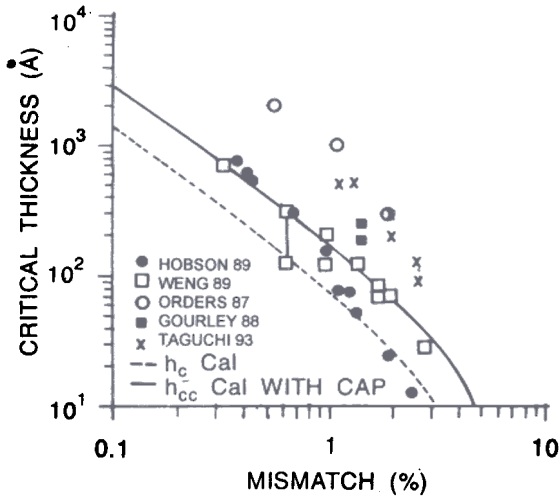


Figure 5. Critical thickness of III-V semiconductor lattice mismatched layers. Dashed and solid lines give the calculated values of  $h_c$  for the layers with free surface and for the capped layers, respectively. The experimental data are taken from Hobson<sup>34</sup>, Weng<sup>35</sup>, Orders<sup>36</sup>, Gurley<sup>37</sup> and Taguchi<sup>38</sup>.

350 °C, the *ZnSe* layers grew in two-dimensional mode. The buffer layers containing 50 - 55 per cent *In* were pseudomorphic with *GaAs* if their thickness was less than 1  $\mu\text{m}$ . Thicker layers showed partial relaxation of strain. The layers were not completely relaxed even when the layer thickness was increased to more than 4  $\mu\text{m}$ . Fontaine, *et al.*<sup>32</sup> studied the strain relaxation in thick uncapped *CdTe* epilayers grown on (111) *Cd<sub>0.96</sub>Zn<sub>0.04</sub>Te* substrates. Lattice mismatch for this system is 0.23 per cent. The experimental values of stress as a function of thickness  $h$  in this case are shown in Fig. 6.

Pinardi, *et al.* have calculated relaxation of strain in thick layers using equilibrium theory. According to this theory, the number of dislocations introduced and the amount of strain relaxed is such that the total energy  $E_T$  of the layer (as a function of dislocation concentration) is minimum. We have made plots of  $E_T$  vs  $1/p$  ( $p$  is the equilibrium spacing) using the equations (6) or (17) for several values of  $h$ . The value of  $p$  at the minimum in these plots give the equilibrium dislocation concentration for each thickness  $h$ . Strain relaxation  $b_1/p$  (Eqn (3)) is then calculated, converted into stress and plotted in Fig. 6. Curve 1 is obtained using Eqn (6) which takes into account interactions properly<sup>11</sup>. Curve 2

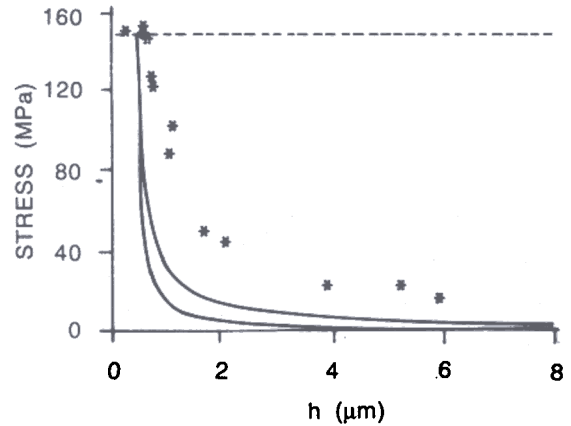


Figure 6. Plots of in-plane stress  $\sigma$  versus layer thickness  $h$  are shown for *CdTe* layers grown on a (111) *Cd<sub>0.96</sub>Zn<sub>0.04</sub>Te* substrate. Symbols are the experimental data taken from<sup>32</sup>. Curve 1 is calculated using Eqn (17) and curve 2 is calculated using Eqn (6) for the total energy of the layer.

uses the old theory based on Eqn (17). The discrepancy between the theoretical data and the experimental data is large. Part of this discrepancy might be attributed to the fact that the samples studied were in (111) orientation, whereas the Eqn (6) or (17) is valid only for (100) substrates.

Petruzzello, *et al.*<sup>8</sup> have investigated the structure of *ZnSe* layers grown on (100) *GaAs* (mismatch 0.27 %) substrate by MBE. High resolution transmission electron microscopy studies showed that there was complete registry of the lattice across the interface. The surface was wavy with an amplitude of about 5 nm. In thin layers ( $h = 50$  nm and 87 nm) stacking faults were observed but there were no misfit dislocations. As the layer thickness increased beyond the experimental  $h_c$  of 150 nm, strain relaxation by the introduction of misfit dislocations began. The measured residual strain in the epilayers of different thicknesses is shown in Fig. 7. The theoretical curves (calculated and discussed earlier) are also shown. The calculated curves have been moved down by  $0.4 \times 10^{-3}$  considering the thermal strain (due to difference in the thermal coefficients of *ZnSe* and *GaAs*). They have been moved to the right by 0.11  $\mu\text{m}$  considering the difference between the calculated  $h_c$  (400 Å) and the observed



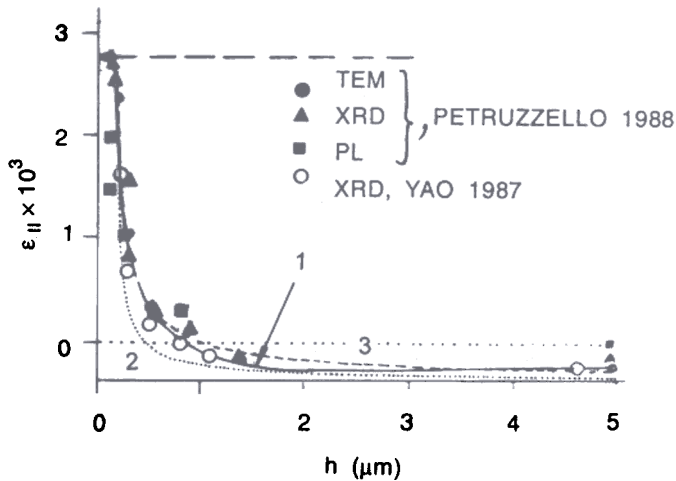


Figure 7. Plots of in-plane strain  $\epsilon_{||}$  in *ZnSe* layers grown on *GaAs*. Curve 1 is drawn through the experimental points shown by symbols (solid symbols are from<sup>8</sup> and open circles are from<sup>30</sup>) as an aid to eye; curve 2 is calculated using Eqn (6) and curve 3 is calculated using Eqn (17) for the total energy.

$h_c$  (1500 Å). The agreement between theory and experiment is quite good in this case.

Yao, *et al.*<sup>30</sup> have measured lattice constant of *ZnSe* grown on (100) *GaAs* (mismatch 0.27 %) substrate. As the thickness of the epilayer was increased, the layers were relaxed by the creation of misfit dislocations at the growth temperature. At the same time on cooling, the in-plane lattice constant increased and lattice constant in the growth direction decreased due to tensile strain caused by the thermal mismatch<sup>30</sup>. Pinari, *et al.* have calculated the strain using their observed values of lattice constants and plotted them by open circles in Fig. 7. For this case also, agreement between theory and experiments is quite good. *ZnSe/GaAs* (100) is the only known case where a reasonable agreement between theory and experiments could be found. The discrepancy between the measured and the calculated strain in the thick *GeSi/Si* and *InGaAs/GaAs* epilayers is very large<sup>11,14</sup>.

## 5. STRAIN RELAXATION IN HIGHLY MISMATCHED LAYERS

If the mismatch between the epilayers and substrate is between 3 and 6 per cent, in many cases the growth is in the Stranski-Krasnov (SK) mode. In the initial stages, the relaxation occurs not by the

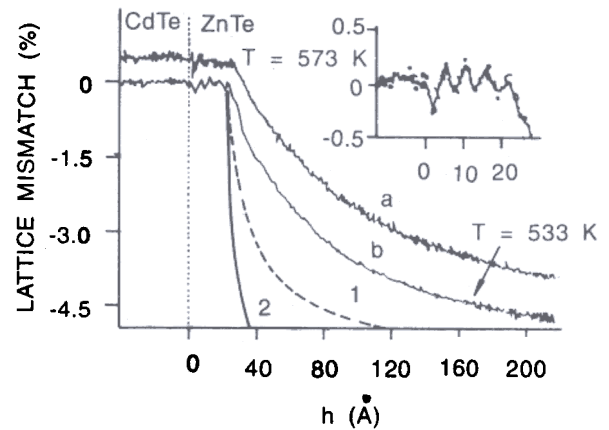


Figure 8. Lattice mismatch of *ZnTe* grown on a *CdTe* relaxed buffer, a and b: experimental results from<sup>29</sup>, curves 1 and 2: strain relaxation calculated using Eqns (6) and (17) for the total energy.

introduction of the misfit dislocations but by formation of islands. Kret, *et al.*<sup>29</sup> have explored the strain relaxation in the early stages of growth of *ZnTe* grown on *CdTe* relaxed buffers (with a mismatch of 5.8 %). The results are compared with the theory (based on relaxation by misfit dislocations) in Fig. 8. The calculated curves (curves 1 and 2) have been moved to the right by  $\sim 18.7$  Å considering the difference between the calculated  $h_c$  ( $\sim 2.3$  Å) and the observed  $h_c$  (21 Å). As expected, the discrepancy between theory and experiments is large. A theory of strain relaxation by the formation and growth of islands does not exist. Figure 8 emphasises the importance of strain relaxation by the islands and the need for developing a theory for this process. The mismatch of *ZnTe* with *GaAs* is 7.5 per cent. In the experiments of Bauer, *et al.*<sup>26</sup> on *ZnTe* epilayers grown on *GaAs* and on *ZnSe/GaAs*, as the thickness is increased beyond  $h_c$  of 12 Å (Table 1), the strain in the layers started to relax. The rate of relaxation was larger in the layers grown directly on *GaAs* substrate. At the thickness  $> 125$  Å, the residual strain became practically constant. In the layers grown on *GaAs* the residual strain was  $-0.4$  but in the layers grown on *ZnSe/GaAs*, it was  $-1.6$ . Residual strain was also determined by measuring average dislocation spacing by HRTEM and the corresponding values were 0.5 and  $-1.7$ . Shift of LO Raman mode in the *ZnTe* layers grown on *ZnSe/GaAs* was larger by  $4 \text{ cm}^{-1}$  wavenumbers which corresponds to an excess strain of  $-1.2$ .

Different techniques give some what different values of strain because they probe different areas and depths of the samples<sup>13</sup>. If it is assumed that the underlying *ZnSe* buffer layers do not relax, these experiments show that chemical nature of the interface plays an important role in determining the relaxation process. This also emphasises the limitation of equilibrium theories of strain relaxation which do not include the nature of the interface.

Schwartzman, *et al*<sup>39</sup>. have made a very detailed study of *CdTe* and *ZnTe* epilayers grown on *GaAs* (100) substrates. The lattice mismatch is 14.6 per cent for *CdTe/GaAs* and 8 per cent for *ZnTe/GaAs* (at these high mismatch values, the exact values depend not only on the lattice constants but also on whether  $a_l$  or  $a_{sub}$  is used in the denominator on the right handside of Eqn (1)). Equilibrium  $h_c$  for these highly mismatched layers is less than 1 atomic layer. Films of a few microns thickness were studied. In such grown films, majority of defects were 60° perfect and dissociated mixed dislocations. There were complicated defects, such as stair-rod dislocations. The dislocation distribution was periodic to a good approximation and the spacing between dislocations in 2  $\mu$ m thick films was 1.64 nm for *CdTe* films and 2.9 nm for *ZnTe* films. Assuming 60° dislocations and using Eqn (7), a residual strain of 0.006 in both cases is obtained. After a long anneal (100 hr at 600 °C), a periodic arrangements of Lomer-edge dislocations was observed. The observed spacing between the dislocations in the annealed samples is shown in Fig. 9. The values calculated are based on the assumption that there are complete relaxation of strain.

$(b_l/p = f_m$  (Eq (3)) are also shown by solid curve. Since edge dislocations cannot glide on (110) planes, they are not directly produced by nucleation. It is now well-known that during the annealing process, two 60° dislocations combine to produce a single edge (90°) dislocation<sup>41</sup>.

In most experiments performed at low mismatch (<1.5 %) the dislocation distribution is not periodic and is highly nonuniform. At high

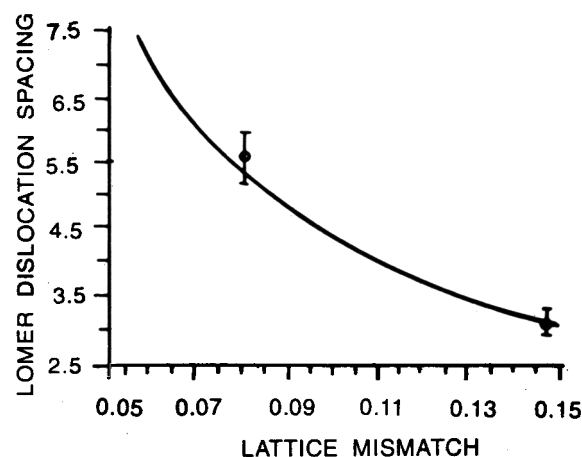


Figure 9. Equilibrium Lomer dislocation spacing (i.e. when there is zero strain) in epilayers as a function of lattice mismatch  $f_m$ . The solid line is the calculated spacing. The points with error bars are the experimentally determined average values for *ZnTe* ( $f_m = 0.08$ ) and *CdTe* ( $f_m = 0.146$ ).

mismatch, the periodic distribution of dislocations seems to be a general feature of all strained layers. In addition to the observation of Schwartzman, *et al*<sup>39</sup>, Kim, *et al*<sup>40</sup>. have observed the periodic distribution in *ZnTe* epilayers grown on *GaAs* (7.5 % mismatch) at 340 °C. In *GeSi/Si* and *InGaAs/GaAs* systems where the maximum lattice mismatch are 4 % and 7 per cent, respectively, a periodic distribution of dislocations is observed when the mismatch is more<sup>11</sup> than 3 per cent.

Pinardi, *et al.* suggest a tentative model which can explain the formation of periodic arrays of dislocations. At low mismatch, the dislocations nucleation is heterogeneous, i.e. it occurs at defects where the energy of activation for nucleation is low. This results in highly clustered or nonuniform distribution of dislocations. At high mismatch, the activation energy for homogeneous nucleation is very small<sup>11</sup> and the loops can nucleate homogeneously and randomly throughout the volume of the film as shown in Fig. 10(a). At this stage, the loops are small in size and are not close to each other. Since the growth is random, the density and the radii of the loops both vary from point-to-point in the layer. Figure 10(b) shows the situation when the loops have grown in size. The loops in the

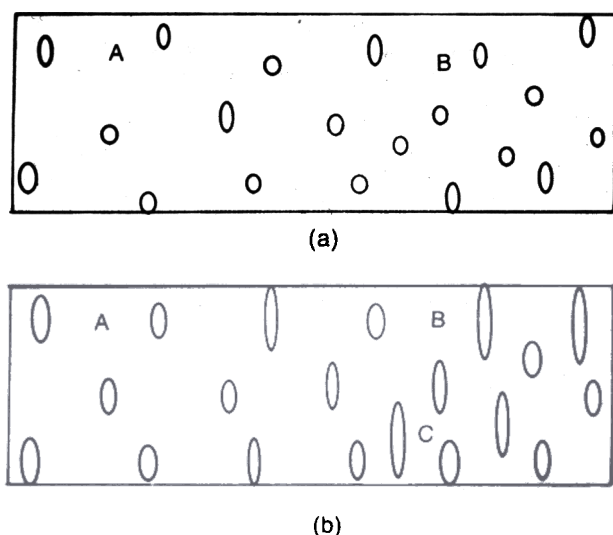


Figure 10. Homogeneous nucleation of loops in a highly mismatched layer (a) shows the state when the loops are small in size and far apart from each other (b) shows that when the loops have grown and some of them, as in region B, have come very close to each other.

region B are bigger and have come very close to each other. The interaction energy of the loops in region B increases rapidly on two counts. Firstly, because the radii of the loops are bigger, and secondly, the loops have effectively come closer to each other. Also, the effective misfit strain in region B has become much smaller than in region A. Because of these two factors, the critical radius for the loops in region B increases. Some of the smaller loops, like loop c in Fig. 10(b) now become subcritical. They will shrink and disappear. Ultimately, only those loops which are approximately at an equilibrium distance and are equal in size, will survive and form a periodic array of misfit dislocations.

## REFERENCES

1. Gunshor, R.L.; Otsuka, N. & Nurmikko, A.V. *IEEE Spectrum*, 1993, Vol (No) pp. 28-33.
2. Gunshor R.L. & Nurmikko, A.V. *Scientific American*, July 1996, Vol (No) pp. 34-37.
3. Hasse, M.A.; Qui, J.; DePuydt, J.M. & Cheng, H. *Appl. Phys. Lett.*, 1991, **59**, 1272-4.
4. Jeon, H.; Ding, J.; Patterson, W.; Nurmikko, A.V.; Xie, W.; Grillo, D.C.; Kobayashi, M. & Gunshor, R. L. *Appl. Phys. Lett.*, 1991, **59**, 3619-21.
5. Yu, Z.; Ren, J.; Lansari, Y.; Sneed, B.; Bowers, K.A.; Boney, C.; Eason, D.B.; Vaudo, R.P.; Gossett, K.J.; Cook, Jr., J.W. & Schetzina, J.F. *Jpn. J. Appl. Phys.*, 1993, **32**, 663-68.
6. Cavus, A.; Zeng, L.; Tamargo, M.C.; Bambha, N.; Semendy, F. & Gray, A. *Appl. Phys. Lett.*, 1996, **68**, 3446-48.
7. Olego, D.J. *Appl. Phys. Lett.*, 1987, **51**, 1422-24.
8. Petruzzello, J.; Greenberg, B.L. & Dalby, R. *J. Appl. Phys.*, 1988, **63**, 2299-303.
9. Yokogawa, T.; Sato, H. & Ogura, M. *Appl. Phys. Lett.*, 1988, **52**, 1678-80.
10. Morinaga, Y.; Okuyama, H. & Akimoto, K. *Jpn. J. Appl. Phys.*, 1993, **32**, 678-80.
11. Jain, S.C. Germanium-silicon strained layers and heterostructures, Advances in electronics and electron physics series, (Supplement 24). Academic Press, Boston 1994.
12. Jain, S.C.; Maes, H.; Pinardi, K. & Wolf, I.De. *J. Appl. Phys.*, 1996, **79**, 8145.
13. Jain, S.C.; Willander, M. & Maes, H. *Semiconductor Sci. Technol.*, 1996, **11**, 641.
14. Jain, S.C.; Harker, A.H. & Cowley, R.A. Advances in Physics (in press).
15. Atkinson, A. & Jain, S.C. *J. Phys. Condens. Matter*, 1993, **5**, 4595-600.
16. Jain, U.; Jain, S.C.; Nijs, J.; Willis, J.R.; Bullough, R.; Mertens, R. & Van Overstraeten, R. *Solid-State Electron.*, 1993, **36**, 331-37.
17. Jain, U.; Jain, S.C.; Atkinson, A.; Nijs, J.; Mertens, R. & Van Overstraeten, R. *J. Appl. Phys.*, 1993, **73**, 1773-80.
18. Martin, R.M. *Phys. Rev.*, 1970, **B 1**, 4005-11.
19. Zogg, H.; Blunier, S.; Fach, A.; Maissen, C.; Muller, P.; Todoropol, S.; Meyer, V.; Kostorz, G.; Dommann, A. & Richmond, T. *Phys. Rev.*, 1994, **B 50**, 10801-10.
20. Swaminathan, V. Indium phosphide and related materials: processing, technology and devices,

- edited by Avishay Katz. Artech House, Boston 1992. p 29.
- 21 Chami, A.C.; Ligeon, E.; Danielou, R.; Fontenille, J.; Lentz, G.; Magnea, N. & Mariette, H. *Appl. Phys. Lett.*, 1988, **52**, 1874-6.
  - 22 Jain, S.C.; Gosling, T.J.; Willis, J.R.; Bullough, R. & Balk, P. *Solid-State Electron.*, 1992, **35**, 1073-9.
  - 23 Ball, C.A.B. & Van der Merwe, J.H. Dislocations in solids, edited by F.R.N. Nabarro, North Holland, 1983. pp. 122-41.
  - 24 Matthews, J.W. Epitaxial growth, Part B, edited by J. W. Matthews. Academic Press, New York, 1975. pp 559-609; J. W. Matthews, *J. Vac. Sci. Technol.*, 1975, **12**, 126-33
  - 25 Cohen-Solal, G.; Bailly, F.; Barbe, M. *J. Crystal Growth*, 1994, **138**, 68-74.
  - 26 Bauer, S.; Huber, M.; Ruth, C. & Gebhardt, W. *Mat. Science Forum*, 1994, **143-147**, 531-36.
  - 27 Faschinger, W.; Juza, P.; Pesek, A. & Sitter, H. *Materials Sci. Forum*, 1994, **143-147**, 1617-662.
  - 28 Cibert, J.; Gobil, Y.; Dang, Le Si.; Tatarenko, S.; Feuillet, G.; Jouneau, P.H. & Saminadayar, K. *Appl. Phys. Lett.*, 1990, **56**, 292-94.
  - 29 Kret, S.; Karczewski, G.; Zakrzewski, A.; Dluzewski, P.; Dubon, A.; Wojtowicz, T.; Kossut, J.; Delamarre, C. & Laval, J.Y. *Acta Physica Polonica*, 1995, **A 88**, 795-98.
  30. Yao, T.; Okada, Y.; Matsui, S. & Ishida, K. *J. Crystal Growth*, 1987, **81**, 518-23.
  31. Cibert, J.; Andre, R.; Deshayes, C.; Feuillet, G.; Jouneau, P.H.; Dang, Le Si.; Mailard, R.; Nahmani, A.; Saminadayar, K. & Tatarenko, S. *Superlattices and Microstructures*, 1991, **9**, 271-74.
  32. Fontaine, C.; Gaillard, J.P.; Magli, S.; Million, A. & Piaguet, gentlemen. *Appl. Phys. Lett.*, 1987, **50**, 903-05.
  33. Lu, K.; Fisher, P.A.; House, J.L.; Ho, E.; Coronado, C.A.; Petrich, G.S.; Hua, G.C. & Otsuka, N. *J. Vac. Sci. Technol.*, **B 12**, 1153-55.
  34. Hobson, G.I.; Khamsehpour, B.; Singer, K.E. & Truscott, W.S. *J. Crystal Growth*, **95**, 220-23.
  35. Weng, S.L. *J. Appl. Phys.*, 1989, **66**, 2217-219.
  36. Orders, P.J. & Usher, B.F. *Appl. Phys. Lett.*, 1987, **50**, 980-82.
  37. Gourley, P.J.; Fritz, I.J. & Dawson, L.R. *Appl. Phys. Lett.*, 1988, **52**, 377-79.
  38. Taguchi, T.; Takeuchi, Y.; Matugatani, K.; Ueno, Y.; Hattori, T.; Sugiyama, Y. & Tacano, M. *J. Crystal Growth*, 1993, **134**, 147.
  39. Schwartzman, A.F. & Sinclair, R. *J. Electronic Materials*, 1991, **20**, 805-14.
  40. Kim, T.W.; Park, H.L. & Lee, J.Y. *Appl. Phys. Lett.*, 1994, **64**, 2526-528.
  41. Jain, U.; Jain, S.C.; Harker, A.H. & Bullough, R. *J. Appl. Phys.*, 1995, **77**, 103-08.

## Contributors

**Dr H E Maes** received his MSc (Electrical Engineering) and PhD both from Katholieke University Leuven, Belgium, in 1971 and 1974, respectively. He worked at various research institutions like Laboratory for Physics and Electronics University of Leuven, Electrical Engineering Research Laboratory, University of Illinois and ESAT Laboratory and University of Leuven during 1971-85. He joined the newly established R&D laboratory of the Interuniversity Micro-Electronics Centre (IMEC) in Belgium, as Head of Analysis and Reliability in 1985. His areas of research include non-volatile memory devices, including ferroelectric memories, physics of semiconductor devices, and integrated circuits, reliability issue and the use of physical techniques in semiconductor related problems. He has been elected, a fellow of the IEEE for his contributions in the field of non-volatile silicon memory devices and MOS reliability physics, wef 1 January 1998. He has authored more than 280 technical papers, some chapters of a book and more than 300 conference papers.

**Dr SC Jain** obtained his MSc (Electronics) from Allahabad University and PhD from University of Delhi, in 1949 and 1955, respectively. He served as Director of Solidstate Physics Laboratory (SPL) and Planning Unit for Research and Training, Ministry of Defence, Delhi, from 1969-84. Since 1985, he has been conducting research at Interuniversity Micro-Electronics Centre (IMEC) in Leuven, Belgium and Oxford University, UK, as Visiting Professor. He was also Visiting Professor at TU Aachen, Germany and University of Tucson AZ, USA. He was honoured with *Shanti Swarup Bhatnagar Award* in 1966 for his outstanding work in physical sciences. He is a member of several learned societies. He has published over 280 papers, authored two books and one patent .

**Dr M Willander** received his PhD (Physics) from the Royal Institute of Technology, Sweden, in 1984. For several years, he worked as Associate Professor at Linköping University, Sweden. Since 1995, he has been working as Professor at Göteborg University/Chalmers University of Technology, Sweden. His areas of research include semiconductor physics and device technology - both theoretical and experimental aspects. He has published a large number of papers in national/international journals.